Clinical Study

Stereotactic and Functional Neurosurgery

Stereotact Funct Neurosurg 2015;93:333–341
DOI: 10.1159/000438997

Received: January 26, 2015
Accepted after revision: July 27, 2015
Published online: September 10, 2015

Metabolic Changes Induced by Electrical Stimulation of Prelemniscal Radiations for the Treatment of Parkinson Disease

Francisco Velasco[a] Sara Llanos[b] Miguel A. Avila-Rodriguez[b]
Arturo Avendaño-Estrada[b] Julián Soto[a] Luis Concha[c]
María Guadalupe García Gomar[c] José D. Carrillo-Ruiz[a, d]

[a]Unit for Stereotactic, Functional Neurosurgery and Radiosurgery, Mexico General Hospital, and [b]PET Unit, National Autonomous University of Mexico Medical School, Mexico City, [c]Institute of Neurobiology, UNAM Campus Juriquilla, Santiago de Querétaro, and [d]Neuroscience and Psychophysiology Coordination, Anahuac University, Huixquilucan, Mexico

Key Words
Parkinson disease · Stereotactic surgery · Posterior subthalamic area · Prelemniscal radiations · Deep brain stimulation · PET/CT

Abstract
Objective: The aim of this work was to study mechanisms of action of electrical stimulation of prelemniscal radiations (Raprl) in the treatment of Parkinson disease, using 2-deoxy-2-fluoro-D-glucose (^{18}F-FDG) Positron Emission Tomography (PET/CT). ***Material and Methods:*** Five patients with PD and predominant unilateral tremor, rigidity and bradykinesia underwent deep brain stimulation (DBS) in contralateral Raprl that improved symptoms from 82.4 to 94.5%. ^{18}F-FDG PET studies were performed before electrode implantation and after DBS therapy. Changes in metabolic activity in PET were evaluated by the maximal standardized uptake value (MSUV) and statistical parametric mapping (SPM) for regions of interest (ROIs) ipsilateral and contralateral to the stimulation site. ROIs were derived from a preoperative probabilistic tractography and included primary motor, supplementary motor and orbitofrontal cortices: Raprl, ventrolateral thalamus, putamen and cerebellum. ***Results:*** No significant MSUV changes occurred in ROIs contralateral to Raprl-DBS. In contrast, MSUV decreased ipsilateral to DBS in Raprl, the thalamus, and the primary and supplementary motor cortices. SPM analysis showed metabolic changes which were significantly different after DBS therapy in all ROIs ipsilateral to DBS compared to those in the contralateral side. ***Conclusion:*** Raprl-DBS decreases the metabolic activity of areas anatomically related to its fiber composition. Improvement of symptoms may result from a decrease in pathological overactivity of circuits related to the ROIs.

Introduction

Deep brain stimulation (DBS) is a well-established therapy for patients with Parkinson disease (PD) who have unsatisfactory control of symptoms or experience side effects with medication. Patients with drug intolerance or early complications may be referred for surgical treatment when symptoms remain prominent only on one side. In such patients unilateral DBS on the side contralateral to the hemi-body showing the most prominent symptoms is indicated.

1011–6125/15/0935–0333$39.50/0

E-Mail karger@karger.com
www.karger.com/sfn

José D. Carrillo-Ruiz, MD, PhD
Periferico Sur 3707-780
Heroes de Padierna
Mexico City 10700 (Mexico)
E-Mail josecarrilloruiz@yahoo.com

Several targets have been effective in controlling motor symptoms of PD, most frequently the subthalamic nucleus (STN), globus pallidus internus (Gpi), and nucleus ventralis intermedius (Vim). While STN-DBS has become the gold standard for surgical therapy because it ameliorates the symptomatic triad of PD, associated cognitive or emotional changes have been reported to complicate this therapy [1–3]. Gpi-DBS is used mainly in rigid and bradykinetic patients as its effect on tremor is less consistent [4], and Vim-DBS is only effective on tremor but does not ameliorate rigidity or bradykinesia [5]. For these reasons, other targets to treat PD are being evaluated.

For many years unilateral PD acral symptoms were successfully treated with lesions [6–9] and more recently with DBS [10–14] of the posterior subthalamic area (PSA). While all reports attest to the efficacy of the PSA-DBS, particularly for tremor, but also for rigidity [11] and bradykinesia [10], there is controversy about the precise location of the optimum target; in some reports DBS is directed to the caudal zona incerta (Zic) [13, 14], while others direct DBS to the prelemniscal radiations (Raprl), which is the white matter region located anterior to the medial lemniscus, medial to Zic, lateral to the red nucleus (Ru) and posterior to the STN [10–12]. The rationale for directing DBS to these fibers is the proven clinical efficacy of such therapy, yet the fiber composition of the Raprl and the possible mechanisms of action of its electrical stimulation have remained obscure. An opportunity to study this mechanism arose from the need to operate on a small group of patients with prominent unilateral symptoms, whose contralateral less affected hemisphere served as a control for the treated side in the image studies. Studies were directed first to demonstrate Raprl fiber composition that might explain why DBS decreased the PD symptomatic triad. Thereafter, we analyzed changes in the metabolic activity of regions of interest (ROIs) induced by DBS, as indirect evidence of neuronal and neuronal fiber activity, evaluated by positron emission tomography coupled with computerized tomography (PET/CT).

Material and Methods

Five patients, 4 males and 1 female aged 43–66 years, who met the UK Parkinson's Disease Society Brain Bank Criteria for idiopathic PD, were selected for the study. None had a family history of PD, encephalitis, or exposure to toxic or neuroleptic drugs. All of the patients presented prominent unilateral tremor, rigidity and bradykinesia that improved over 30% in the Unified Parkinson's Disease Rating Scale (UPDRS) part III (motor) score by administration of L-DOPA/CARBIDOPA 500 mg/day. They were classified as Hoehn-Yahr stage 1.5–2.5 OFF medication; their symptoms were prominent on the right side in 4 cases and on the left side in 1 case. They were considered for surgical treatment because initial improvement with L-DOPA was complicated by motor fluctuations (1 case) or was associated with dyskinesia (2 cases) or with intolerance to the medication (2 cases). Patients were stereotactically implanted with tetrapolar electrodes for DBS (DBS-3387, Medtronic Inc., Minneapolis, Minn., USA) directed to the Raprl in the PSA contralateral to the most prominent symptoms, as described previously [8, 10, 11, 15]. Briefly, stereotactic coordinates for indirect targeting were 2/10 the length of the intercommissural (AC-PC) line in front of the anterior border of posterior commissure; 2/10 below the AC-PC level and 4.5/10 lateral to the midsagittal plane. Direct targeting oriented electrodes to the white matter adjacent to the lateral border of Ru and posterior-medial to the internal border of STN (fig. 1a). Microelectrode recordings guided the placement of DBS electrodes in the posterior subthalamic region onto fibers that compose the Raprl [15]. Transoperative macrostimulation confirmed the effect of DBS on tremor, rigidity and bradykinesia, which in 4 cases improved with the simple insertion of the electrode. Correct positioning of the electrodes on the intended target was confirmed by postimplantation 1.5-tesla MRI, performed before internalization of the neurostimulation system (fig. 1a).

The following day bipolar stimulation was performed through different adjacent contacts of electrodes in a free moving session for deciding the pair of contacts that would be used for chronic stimulation, on the basis of a lower current amplitude for symptom control and a higher threshold for adverse events. Electrical stimulation was set at 130 Hz, 90–120 μs, 1.5–2.5 V, bipolar between a pair of adjacent contacts, usually contacts 1–2 [15]. Contralateral symptoms improved in all patients, and after DBS was optimized (2–3 months) the UPDRS motor score decreased by 82.4–94.5% on the contralateral side (table 1).

MRI Acquisition

Prior to the surgical procedure, patients underwent a 3-tesla MRI scanning session (Philips Achieva TX, Best, The Netherlands) in which diffusion-weighted images (DWI) were acquired using a single-shot echo-planar imaging sequence with 120 unique, diffusion-encoding gradient directions with b = 2,000 s/mm^2 (along with 4 non-DWI, b = 0 s/mm^2), with a voxel resolution of 2 × 2 × 2 mm^3. During the same imaging session high-resolution (1 × 1 × 1 mm^3) anatomical volumes were acquired with T1 and FLAIR-T2 contrasts. Constrained-spherical deconvolution [16, 17] was performed on the DWI datasets, which estimates the diffusion profile in each voxel, indicating the relative contribution of diffusion in different directions, even in areas of crossing fibers. Then, track-density images (TDI) [18] were computed based on the probabilistic tractography of one million seeds distributed uniformly across the whole brain. TDI dramatically improves the working spatial resolution by an order of magnitude, namely to 0.25 × 0.25 × 0.25 mm^3, and increases the visibility of subthalamic subregions. The resulting TDI, along with the coregistered anatomical images, were used for the careful manual segmentation of the PSA by a single operator (M.G.G.-G.; fig. 1b).

Raprl segmentations were used as seed regions for the propagation of 50,000 streamlines, which were then further subdivided based on their destinations. Regions that showed anatomical connectivity with the Raprl included the primary motor cortex (PMC),

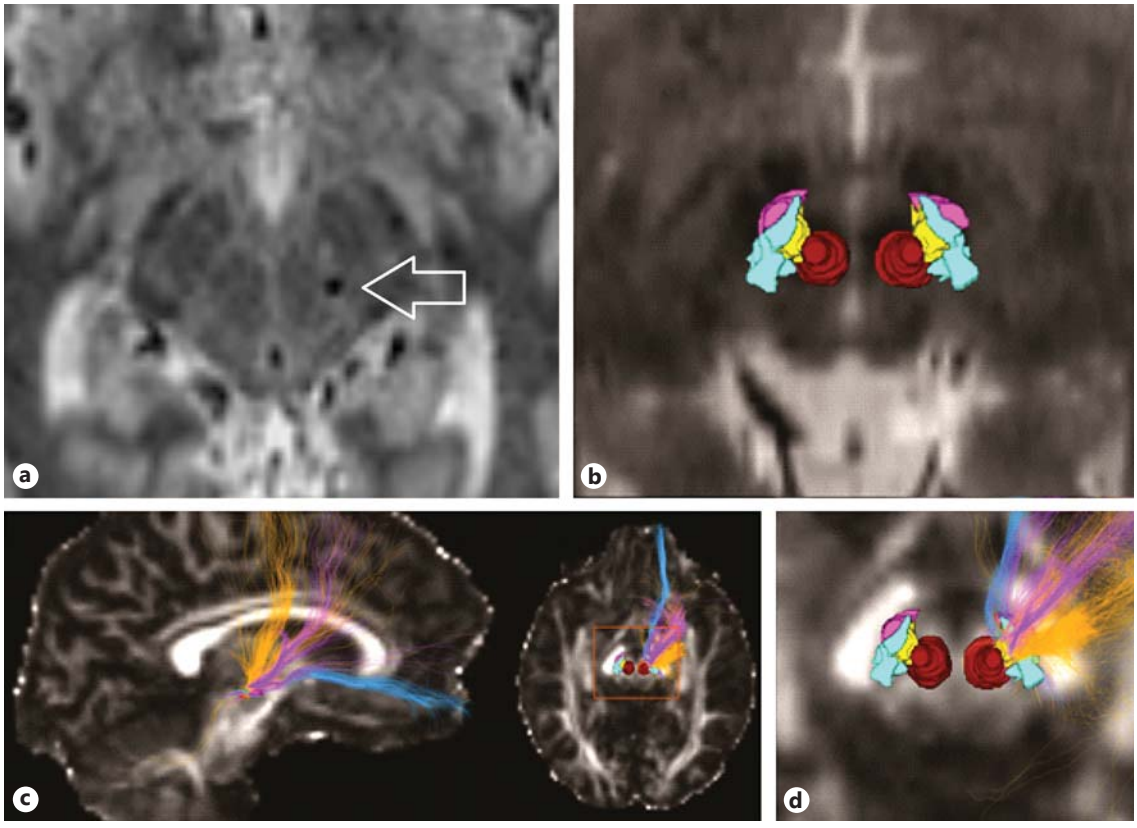

Color version available online

Fig. 1. a Stereotactic placement of a DBS electrode in Raprl in a postoperative axial T2 MRI of a representative case (patient 1) at the level of the superior colliculus. The electrode (arrow) is behind the posterior margin of the STN, lateral to the anterior pole of the Ru, and medial to the caudal Zic. **b** preoperative axial T2 MRI at the same level as in **a** with segmentation of different anatomic structures identified by colors: Ru = red, STN = pink, Zic = cyan, Raprl = yellow. **c** Probabilistic tractography of Raprl overlapped in a fractional anisotropy map. In the left image a sagittal view of three main components can be identified: cerebellar-thalamic-cortical (orange), Gpi-PPN (purple) and orbitofrontal-mesencephalic components (blue). This pattern was found in all patients. The right image shows an axial view of these fiber bundles and the anatomical segmentation of structures within the PSA; the rectangle indicates the area enlarged in **d**, illustrating the convergence of fibers as they traverse Raprl.

supplementary motor area (SMA) and orbitofrontal cortex (OFC), ventrolateral thalamic nuclei (Th) and cerebellum (Cer) [19] (fig. 1b, c). From this connectivity pattern, these anatomical regions were taken as ROIs for the present study. Since in 3 patients the visual examination of images detected decreased metabolism in the posterior putamen (Pu) contralateral to the most prominent symptoms, as has been reported for idiopathic PD [20], this structure was also included as a ROI. Connectivity of the Raprl to the pedunculopontine nucleus (PPN) and globus pallidum was also observed, but these regions were not analyzed as they were not visible on either PET or CT.

PET/CT Imaging Acquisition

Patients had ^{18}F-FDG PET scans 2–6 weeks prior to implantation of the DBS electrode and again 3–4 months after implantation, by which time DBS programming had reached its optimal level. PET scans were obtained using a high-resolution lutetium orthosilicate crystal biograph 64 PET, coupled to a 64-slice CT scanner (Siemens Healthcare, Freiburg Germany). L-DOPA administration was discontinued 12 h before each study. Studies were performed between 8.00 and 10.00 a.m. after 8 h of fasting and 12 h after discontinuing L-DOPA administration. Prior to the study a peripheral vein was canalized and 370 MBeq of FDG was administered as a 10-ml solution in saline. Patients remained resting in a room with dimmed lights, without visual or auditory stimuli for 30 min prior to the study. Thereafter, they were positioned in the PET/CT scanner in decubitus, with the head oriented through a three-dimensional laser aligned parallel to the canto-meatal line for axial views and to the midsagittal plane for sagittal sections, and restrained with elastic bands to avoid motion. An anesthesiologist accompanied patients throughout the study to detect any voluntary or involuntary head movements. The emission scan was acquired for 8 min (128 × 128 matrix), and PET data were reconstructed using an ordered-subsets expectation maximization algorithm (three iterations, fourteen subsets) and a Gaussian filter. CT data were used for attenuation correction and anatomic localization. CT images were acquired using a plain cranial protocol at 380 mA/s, 120 kilovoltage peak (kVp) and and 1.0-second tube rotation time. Slice thicknesses were 4.0 mm for PET and 2.0 mm for CT images.

Table 1. Demography of cases

Initials	Sex	Age, years	Years PD	Contralateral symptoms	Ipsilateral symptoms	Implanted side	Contralateral improvement (6 months)	Δ contralateral symptoms, %	UPDRS pre/post	Hoehn-Yahr pre/post
LFC	M	54	5	T = 6 R = 4 B = 6	T = 1 R = 0 B = 0	L	T = 0 R = 0 B = 2	–87.5	42/29	2.5/1.5
ELL	M	66	2	T = 7 R = 4 B = 6	T = 0 R = 1 B = 2	L	T = 1 R = 1 B = 2	–82.4	37/15	2.5/1.0
FTR	F	54	2	T = 2 R = 4 B = 12	T = 0 R = 2 B = 2	L	T = 0 R = 0 B = 3	–83.3	60/33	2.5/2.0
RRB	M	43	3	T = 6 R = 4 B = 7	T = 4 R = 2 B = 3	L	T = 0 R = 0 B = 3	–82.4	36/20	1.5/1.0
CPB	M	43	3	T = 6 R = 4 B = 8	T = 0 R = 2 B = 0	R	T = 0 R = 1 B = 0	–94.5	39/8	1.5/0.5
Mean	–	52	3	T = 5.4 R = 4.0 B = 7.8	T = 1.0 R =1.4 B =1.4	–	T = 0.2 R = 0.4 B = 2.0	–86.02	42.8/21	2.3/1.2

The severity of symptoms were evaluated by UPDRS Part III (motor) on a scale of 0–4 for each extremity on each side for items 20–21 (tremor; T), 23 (rigidity; R) and 24–27 (bradykinesia; B). Years PD = Years since PD was diagnosed; Δ% = decreased (–) or increased (+) percentage from the baseline evaluation, OFF medication condition; UPDRS pre/post = global Unified Parkinson's Disease Rating Scale score before and after DBS treatment, OFF medication.

Semiquantitative Analysis

For comparative analysis between pre- and postoperative studies, images were realigned and normalized in a stereotactic space using as a reference the AC-PC line. PET images were smoothed by applying a Gaussian filter of 7 mm FWHM (full width at half maximum) to improve the signal-to-noise ratio.

Semiquantitative analysis was performed using the maximal standardized uptake value (MSUV) measured through the imaging software OsiriX MD v.1.0 (Pixmeo SARL, Geneva, Switzerland). Since visual inspection detected a decrease in the size of metabolically active areas for the ROIs on the side of Raprl-DBS (see results and fig. 2), the metabolic areas were delineated for each ROI in all studies on both hemispheres and their extension measured through the same software and reported in square centimeters.

CT studies allowed the differentiation of gray from white matter, so the number of sections analyzed for each ROI depended on their thickness of gray matter, except for Raprl, which is white matter of about 7-mm dorsoventral thickness below the posterior third of the AC-PC line. Therefore, consecutive PET/CT 4.0-mm-thick sections were analyzed as follows: 4 sections for PMC starting from the convexity down; 4 sections for SMA starting from the upper border of the cingulate gyrus up; 3 sections of the ventral thalamus starting from the AC-PC level up; 2 sections for Raprl starting from the AC-PC level down; 4 sections of the Pu from its lower margin up; 3 sections for the OFC from its ventral surface up, and 4 sections for the Cer.

Differences in readings for MSUV and the extension of metabolic active areas for each ROI were compared in the following conditions: (i) ipsilateral versus contralateral to Raprl-DBS in preoperative studies; (ii) ipsilateral versus contralateral to Raprl-DBS in postoperative studies; (iii) ipsilateral to Raprl-DBS in pre- versus postoperative studies; (iv) contralateral to Raprl-DBS in pre- versus postoperative studies. This last analysis provided evidence of interstudy variability. The significance of changes was determined by the dependent paired Student t test.

Quantitative Analysis

In the 4 subjects operated on the left hemisphere, a voxel by voxel analysis between pre- and post-Raprl-DBS images was performed using statistical parametric mapping (SPM; v. 8.0) in MATLAB 2013_B (Mathworks, Natick, Mass., USA). Intersubject coregistration was performed using rigid body transformation in 3 translations and 3 rotations along different axes on a reference image. Each individual brain image was normalized on an anatomical atlas to be compared within a standard space (International Consortium for Brain Mapping). Images were smoothed by applying a Gaussian filter of 7 mm FWHM to improve the signal-to-noise ratio. Since the number of subjects was small, a nonparametric permutation test providing family-wise error-corrected in-

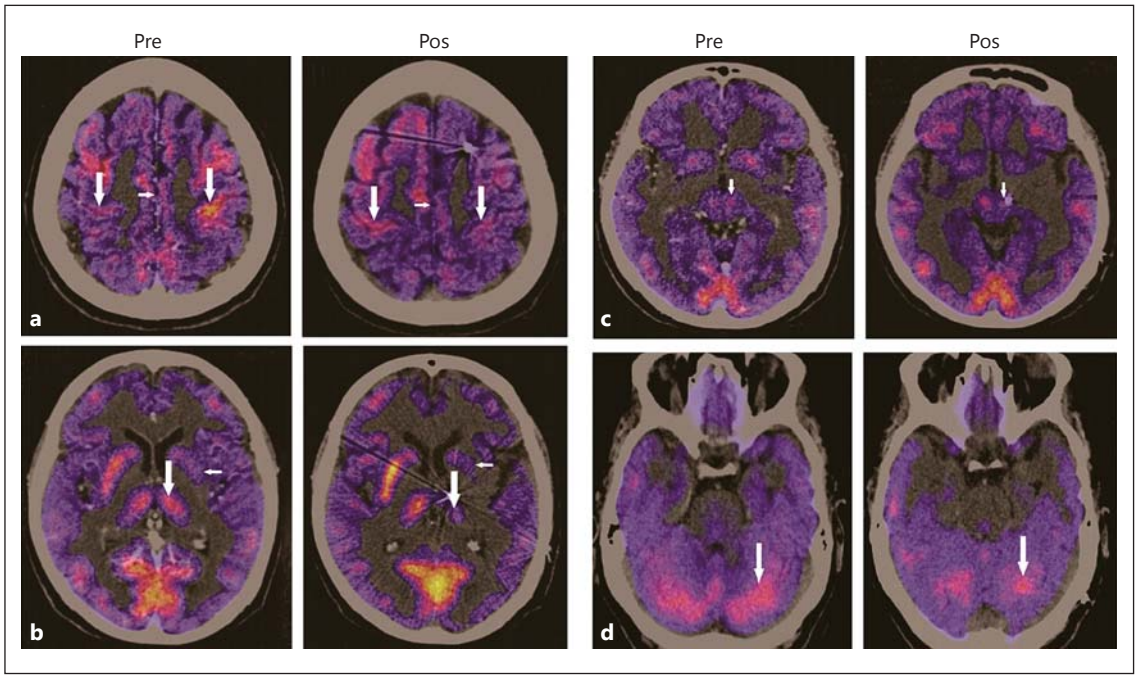

Fig. 2. Preoperative (Pre) and postoperative (Pos) PET/CT using FDG. **a** A cortical axial section showing a larger metabolically active area of the left PMC as compared with the right PMC (vertical arrows) in the preoperative study, and its decrease in the postoperative study ipsilateral to the Raprl-DBS. The metabolically active area in the SMA is also decreased by Raprl-DBS (horizontal arrow). **b** A PET/CT section at the level of the Th (vertical arrow) and Pu (horizontal arrow). Notice that Pu MSUV and the metabolically active area are decreased on the left side in the preoperative study, while both sides are similar for Th. The postoperative study shows the MSUV and metabolically active area to be decreased in the Th on the side of Raprl-DBS (vertical arrow), while they remain similar on the contralateral side. The Pu metabolically active area is reduced on the left in both the preoperative and postoperative studies (horizontal arrow). **c** A preoperative axial section at the level of the subthalamic region shows similar uptake on both sides (arrow), while it is decreased on the side of stimulation in the postoperative study. **d** The MSUV and metabolically active area are similar on both sides of the Cer and decrease bilaterally after left Raprl-DBS.

ferences was performed, using an SPM extension (SnPM). A paired t test between pre- and post-DBS images was carried out ($\alpha = 0.05$). A statistical parametric map between Raprl-DBS studies was obtained (fig. 3). On this map, 10 intensity voxel values per region (PMC, SMA, Th, Pu, OFC, Cer) were compared for ipsi- versus contralateral Raprl-DBS hemispheres. The mean of signal intensity in each region was compared with a paired t test ($\alpha = 0.05$) to its contralateral homologous region.

Results

From the analysis of probabilistic fiber tracts derived from MRI-DWI studies, three major components of Raprl were identified: cerebellar fibers from both the contralateral and ipsilateral cerebellar cortex and deep cerebellar nuclei traveling in the brachium conjunctivum towards the ventrolateral thalamus (Th), and from there to the PMC and SMA; a second component derives from fibers of the ansa lenticularis that extend beyond Forel's fields, passing above the STN towards the brain stem, at the level of the pons in a space between the brachium conjunctivum and medial lemniscus, most likely the PPN, and a third bundle connects the OFC with the mesencephalic tegmentum (fig. 1c) [19].

In visual analysis of pre- versus postoperative PET/CT studies, a decrease in metabolic activity in postoperative studies over the PMC and SMA ipsilateral to Raprl-DBS was evident, while it remained unchanged in the contralateral hemisphere (fig. 2a, arrows). Thalamic metabolism decreased considerably on the side of Raprl-DBS (fig. 2b, vertical arrow), while no changes were seen on the contralateral side. The metabolically active area and MSUV of Pu was decreased in the preoperative study on the side of DBS and remained so in post-DBS studies (fig. 2b, horizontal arrow). Metabolic activity also decreased in the ipsilateral subthalamic region where DBS was applied (fig. 2c). Figure 2d shows the MSUV decrease in both cerebellar hemispheres.

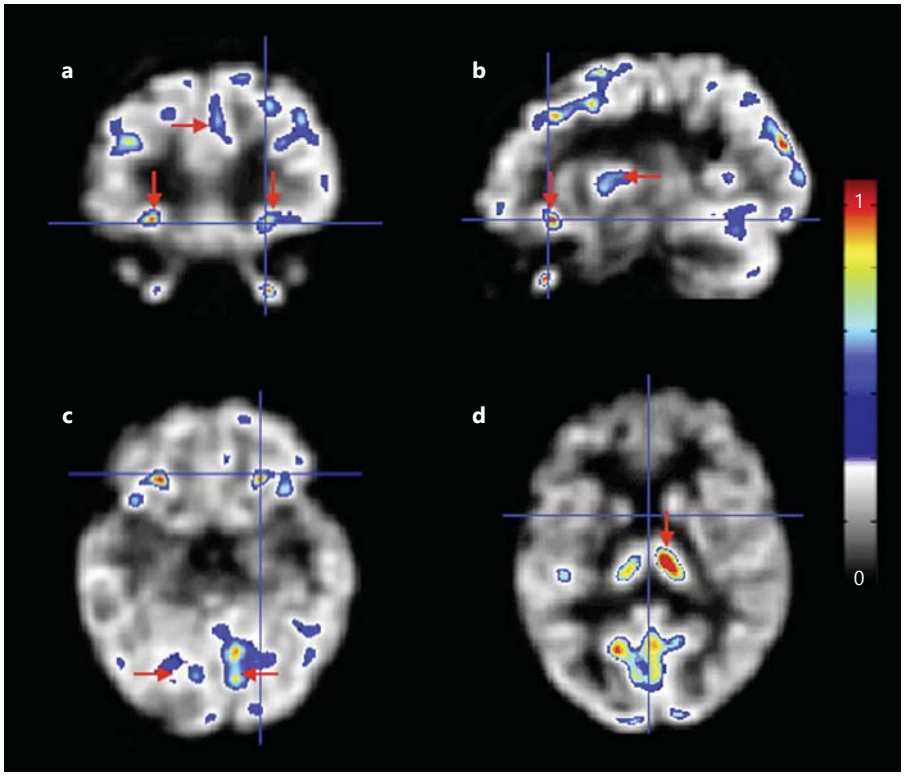

Fig. 3. SPMs show the metabolic changes between pre- and postoperative studies normalized to one (1) for the area with major change. Hot spots are indicated in red and include: OFC (vertical arrows) and SMA (horizontal arrow) in the coronal section (**a**), OFC (vertical arrow) and Pu (horizontal arrow) in the sagittal section (**b**), OFC and Ce on both sides (horizontal arrows) in the axial section below the AC-PC level (**c**) and in the thalamus (above the AC-PC level; arrow; **d**).

Table 2 summarizes the semiquantitative analysis for each ROI as follows: (i) in preoperative studies, no significant differences in the metabolically active area or MSUV of ROIs were found between the side to be stimulated and the contralateral hemisphere, except for a decreased area and MSUV in the Pu of the hemisphere contralateral to the more prominent symptoms ($p = 0.01$ for the area and 0.00008 for MSUV); (ii) compared with the nonstimulated side, postoperative studies showed a significant decrease on the side of Raprl-DBS of MSUV in the PMC ($p = 0.001$) and Raprl ($p = 0.00004$), and decrease of both the metabolically active area and MSUV in the thalamus ($p = 0.00003$ and $p = 0.0014$, respectively) and Pu ($p = 0.00002$ and 0.00016, respectively); (iii) comparing the ROIs ipsilateral to Raprl-DBS between pre-and postoperative studies, there was a significant decrease in the metabolically active area in the PMC ($p = 0.0002$), SMA ($p = 0.005$), Th ($p = 0.00001$) and Raprl ($p = 0.05$), but not in other ROIs, whilst MSUV values remained unchanged; (iv) in contrast, there were no significant changes in either the metabolically active area or MSUV in homologous ROIs in the hemisphere contralateral to Raprl-DBS between pre- and postoperative studies, except for a borderline postoperative increase in Pu MUSV.

The imaging analysis with SPM did not show statistically significant differences ($\alpha = 0.05$) between pre- and post-DBS images. However, since the parametric mapping showed regions with higher and lower metabolic changes, a supplementary analysis that compared the metabolic activity of a 10-voxel cluster focused in the center of each ROI ipsi- and contralateral to Raprl-DBS was performed, generating a parametric map of metabolic changes expressed on a scale of hot (yellow to red) to cold (black to blue) colors. The results are expressed in a scale of values normalizing to one (1) for the area with higher metabolic change (fig. 3). The significance of these changes was evaluated by the paired Student t test. Figure 4 is a box plot that compares median values of normalized changes of metabolic activity for ipsi- and contralateral Raprl-DBS for each ROI. Significant differences were found in all ROIs ($p < 0.0001$).

Discussion

As reported here and previously, patients treated with Raprl-DBS show considerable improvement in motor symptoms of PD, including tremor, rigidity and bradykinesia contralateral to DBS [10, 12], but the underlying mechanism of improvement has remained speculative up to the present. With emerging imaging techniques, such

Table 2. Semiquantitative analysis for each ROI

		I stim pre/no stim pre		II stim post/no stim post		III stim pre/stim post		IV no stim pre/no stim post	
ROI		area	MSUV	area	MSUV	area	MSUV	area	MSUV
PMC (n = 20)	MSUV	2.09/1.88	6.46/6.46	1.10/1.76	6.02/6.48	2.09/1.10	6.46/6.02	1.88/1.76	6.46/6.48
	SD	0.8/0.5	1.0/1.1	0.6/0.7	0.6/0.6	0.8/0.6	1.0/0.6	0.5/0.7	1.0/0.6
	p	0.22	0.91	0.44	**0.001**	**0.0002**	0.2	0.2	0.94
SMA (n = 20)	MSUV	1.29/1.30	6.28/6.33	0.81/1.04	6.36/6.39	1.29/0.81	6.28/6.36	1.30/1.04	6.33/6.39
	SD	0.6/0.6	0.4/0.7	0.4/0.7	0.7/0.7	0.6/0.4	0.4/0.7	0.6/0.7	0.7/0.7
	p	0.94	0.5	0.13	0.7	**0.005**	0.7	0.14	0.77
Th (n = 15)	MSUV	1.35/1.41	6.59/6.46	0.52/1.19	6.02/6.48	1.35/0.52	6.59/6.02	1.41/1.19	6.46/6.48
	SD	0.4/0.4	1.0/0.6	0.2/0.3	0.6/0.7	0.4/0.2	1.0/0.6	0.4/0.3	0.6/0.7
	p	0.2	0.07	**0.00003**	**0.0014**	**0.00001**	0.08	0.97	0.08
Raprl (n = 10)	MSUV	0.34/0.31	5.52/5.46	0.06/0.28	5.06/5.86	0.34/0.06	5.52/5.06	0.3/0.28	5.46/5.86
	SD	0.1/0.1	0.8/0.7	0.1/0.1	0.07/0.06	0.1/0.1	0.8/0.7	0.1/0.1	0.7/0.6
	p	0.27	0.4	0.7	**0.00004**	**0.05**	0.06	0.24	0.23
Pu (n = 20)	MSUV	2.26/2.71	6.68/7.11	1.97/2.83	6.49/7.6	2.26/1.97	6.68/6.99	2.71/2.83	7.1/7.6
	SD	1.0/1.0	0.4/0.4	0.8/0.6	0.9/0.6	1.0/0.8	0.4/0.9	1.0/0.6	0.4/0.6
	p	**0.01**	**0.00008**	**0.00002**	**0.00016**	0.06	0.3	0.93	**0.05**
CER (n = 20)	MSUV	6.12/7.96	5.86/6.14	7.96/9.2	6.12/6.12	6.12/7.96	5.86/6.12	7.96/9.2	6.14/6.12
	SD	2.8/3.3	0.7/0.8	4.1/5.4	1.2/1.4	2.8/4.1	0.7/1.2	3.3/5.4	0.8/1.4
	p	0.15	**0.01**	0.21	0.4	0.06	0.5	0.11	0.88
OFC (n = 15)	MSUV	2.1/1.8	5.6/5.6	1.9/2.3	5.7/5.5	2.1/1.9	5.6/5.7	1.8/2.3	5.6/5.5
	SD	1.2/1.2	0.8/0.9	0.9/1.6	1.2/1.4	1.2/0.9	0.8/1.2	1.2/1.6	0.9/1.4
	p	0.08	0.8	0.3	0.4	0.5	0.4	0.7	0.9

With each ROI the number of readings included in statistical analysis (n) is provided for each side. Readings of MSUV and metabolically active area (cm^2) were provided automatically by OsiriX MD software. The following comparisons were performed for each ROI: I, the side to be stimulated by DBS against the side not to be stimulated in the preoperative study; II, the stimulated against the not stimulated side in the postoperative study; III, pre- against poststimulation value in the stimulated hemisphere; IV, pre- against post-DBS on the nonstimulated side. Notice that changes became significant in the stimulated hemisphere for PMC, SMA, Th and Raprl in columns II and III, but not in IV. SD = Standard deviation; p = probability value for each ROI (with significant values indicated in bold).

as super-resolution track-density imaging and constrained spherical deconvolution [16, 18], analysis of short tracts and fiber composition of crossing fiber tracts became possible. Probabilistic tracts seem to be related to different anatomical circuits, and abnormal activity in each fiber tract may be related to different symptoms of PD [19].

It is evident that the major limitation of the present study is the number of patients included in the analysis. However, changes in PET studies are strongly supported by semiquantitative and quantitative automated methods. Metabolic changes revealed by MSUV and extension of the metabolic active area were significant only in the ROIs of the hemisphere where Raprl-DBS was applied, and not in the contralateral hemisphere. Quantitative analysis of changes by SPM confirmed that metabolic activity was significantly different between ROIs ipsilateral and contralateral to DBS. Therefore, we assume changes were induced by DBS. Metabolic activity as revealed in ^{18}F-FDG PET studies has been correlated with the degree of neuronal activity in a given area, while increased metabolism indicates increased neuronal activity and decreased metabolism indicates the opposite [21].

The results herein presented may provide insight into the mechanism of action of Raprl-DBS in controlling PD symptoms. We must keep in mind that the stimulated area is composed of fibers and not of nuclei, as determined by structural MRI (fig. 1) and transoperative microelectrode recordings [22]. Assuming that regional metabolic activity is indirect evidence of neuronal activity, Raprl-DBS would inhibit local fibers and areas ana-

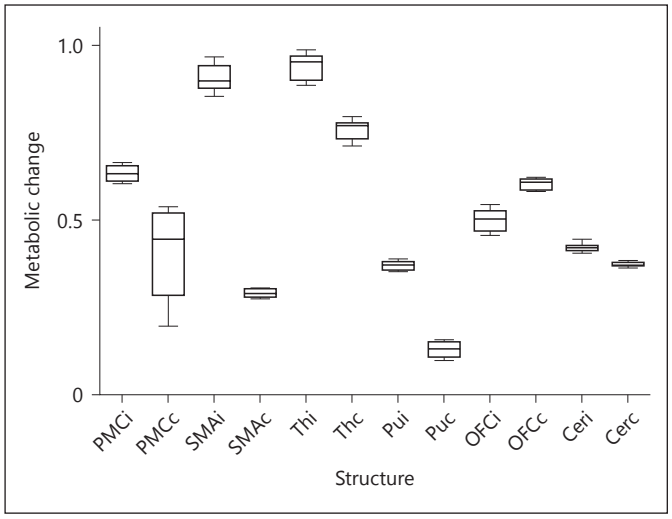

Fig. 4. Box plots of median values of normalized metabolic changes for ROIs of 10-voxels each ipsilateral (i) and contralateral (c) to Raprl-DBS. The significance threshold was set at $\alpha = 0.05$; all contralateral ROIs were significantly different from ipsilateral ROIs ($p < 0.0001$).

tomically connected through such fibers, i.e. the ventral Th, PMC, SMA and Cer.

At the level of Raprl, electrical stimulation decreased mainly MSUV, which indicates that high-frequency stimulation (HFS) of fibers inhibits the activity of fiber bundles. This contrasts with the hypothesis that HFS has a dual effect: on the neuronal body it is inhibitory, while on axons it is excitatory [23, 24], and it is different from what has been reported for STN-DBS [25]. Inhibition is transmitted downstream to the Th, where both the metabolically active area and MSUV is decreased relative to the contralateral postoperative Th (see table 2, 'Th' columns II and III). Inhibition continues downstream to the PMC where the metabolically active area is decreased compared to the preoperative ipsilateral PMC (see table 2, column III). This effect raises a question about the pathophysiological role of thalamic inhibition in the development of motor symptoms of PD and the role of DBS-induced Gpi inhibition in releasing thalamic-cortical activity [26, 27]. A decrease in PMC activity by Raprl-DBS resembles what has been reported in PET scans when treating generalized tardive dystonia by Gpi-DBS, where generalized pathological cortical overactivity is decreased and reset to normal levels correlating with improvement of dystonic movements [28]. Reduced PMC overactivity has also been identified by ^{18}F-FDG PET after administration of L-DOPA, correlating with a decrease in tremor amplitude in PD patients [29]. In our cases, a decrease in the PMC metabolically active area may be related to the decrease in pathological activity responsible for tremor. Studies evaluating the effect of DBS of the STN (STN-DBS) on metabolic activity and regional cerebral blood flow (rCBF) by PET scans have reported decreases in both metabolic activity and rCBF in the PMC associated with STN-DBS [30–33].

At the level of the SMA the metabolically active area ipsilateral to Raprl-DBS was significantly decreased relative to the preoperative value. Reductions in metabolic activity and rCBF in the SMA as seen in PET have also been reported for STN-DBS and correlated with an improvement of rigidity [34], although in some studies no significant changes occurred [35], and in others activity was even increased [36]. In our cases, the reduction in the metabolically active area of SMA may have a similar impact on rigidity as that in the PMC has on tremor.

In contrast, low preoperative metabolic activity (area and MSUV) in the Pu contralateral to the most prominent symptoms decreased even more after Raprl-DBS when compared to the nonstimulated side. To determine if this indicates that Raprl-DBS does not act by restoring normal striatal activity in PD patients will require future studies using specific radiotracers linked to dopamine metabolism.

Cerebellar and orbitofrontal MSUV did not present significant changes in the semiquantitative analysis; however, SPM analysis indicated that there were significant bilateral changes in both structures. In the OFC, contrary to all other ROIs, the change is greater contralateral to Raprl-DBS.

PPN and Gpi were not analyzed due to the difficulty in locating these structures in PET/CT studies. With additional information on the location of endings of fiber tracts conforming Raprl, derived from MRI-DTI studies of more PD patients and controls, a profile of these ROIs is being delineated for future PET studies coupled with MRI.

Conclusion

Highly effective control of acral symptoms in PD patients by Raprl-DBS is associated with decreased metabolic activity of fibers conforming Raprl, which may indicate decreasing fiber electrophysiological activity. This inhibition extends downstream towards anatomically related Th and cortical areas, as well as the Cer. Observations suggest that HFS of fiber tracts caused the same inhibitory effect as HFS in neuronal soma and that the improvement of symptoms is related to the suppression of pathological hyperactivity in anatomically connected structures.

References

1 Woods SP, Fields JA, Troster AI: Neuropsychological sequelae of STN-DBS in Parkinson's disease: a critical review. Neuropsychol Rev 2002;112:111–126.
2 Funkiewiez A, Ardouni C, Caputo E, Krack P, Fraix V, Klinger H, Chabardes S, Foote K, Benabid AL, Pollak P: Long-term effects of bilateral subthalamic nucleus stimulation on cognitive function mood and behavior in Parkinson's disease. J Neurol Neurosurg Psychiatry 2004;75:834–839.
3 Hershey T, Revilla FJ, Wemle A, Gibson PS, Dowling JL, Perlmutter JS: Stimulation of STN impairs aspects of cognitive control in PD. Neurology 2004;62:1110–1114.
4 Jimenez F, Velasco F, Carrillo-Ruiz JD, Garcia L, Madrigal A, Velasco AL, Marquez I: Comparative evaluation of the effects of unilateral lesion versus electrical stimulation of the globus pallidum internus in advanced Parkinson's disease. Steretact Funct Neurosurg 2006;84:64–71.
5 Benabid AL, Pollack P, Gervason C, Hoffman D, Gao DM, Hommel M, Perret JE, De Rougement J: Long-term suppression of tremor by chronic stimulation of ventral intermediate thalamic nucleus. Lancet 1991;337:403–406.
6 Mundinger F: Stereotaxic interventions on the zona incerta area for treatment of extrapyramidal motor disturbances and their results. Confin Neurol 1965;26:222–230.
7 Bertrand C, Hardy J, Molina-Negro P, Martinez SN: Optimum physiological target for the arrest of tremor; in Gillingham JF, Donaldson JML (eds): 3rd Symposium on Parkinson's Disease. Edimburgh, Livingstone, 1969, pp 251–254.
8 Velasco F, Molina-Negro P, Bertrand C, Hardy J: Further definition of the subthalamic target for tremor arrest. J Neurosurg 1972;36: 184–191.
9 Ito Z: Stimulation and destruction of the prelemniscal radiation or its adjacent area in various extrapyramidal disorders. Confin Neurol 1975;37:41–48.
10 Velasco F, Jimenez F, Perez ML, Carrillo-Ruiz JD, Velasco AL, Ceballos J, Velasco M: Electrical stimulation of the prelemniscal radiation in the treatment of Parkinson's disease: an old target revised with new techniques. Neurosurgery 2001;49:293–304.
11 Kitagawa M, Murata J, Uesegi H, Kikuchi S, Saito H, Tashiro K, Sawamura Y: Two-year follow-up of chronic stimulation of the posterior subthalamic white matter for tremor dominant Parkinson's disease. Neurosurgery 2005;56:281–289.
12 Carrillo-Ruiz JD, Velasco F, Jimenez F, Castro G, Velasco AL, Hernandez JA, Ceballos J, Velasco M: Bilateral electrical stimulation of pre-lemniscal radiations in the treatment of advanced Parkinson's disease. Neurosurgery 2008;62:347–357.
13 Plaha P, Ben-Shlomo Y, Patel NK, Gill SS: Stimulation of the caudal zona incerta is superior to stimulation of the subthalamic nucleus in improving contralateral parkinsonism. Brain 2006;129:1732–1747.
14 Blomstedt P, Fytagoridis A, Tisch S: Deep brain stimulation of the posterior subthalamic area for the treatment of tremor. Acta Neurochir 2009;151:31–36.
15 Velasco F, Palfi S, Jimenez F, Carrillo-Ruiz JD, Castro G, Keravel Y: Other targets to treat Parkinson's disease: posterior subthalamic area and motor cortex; in Lozano AM, Gildenberg PI, Tasker RR (eds): Textbook of Stereotactic and Functional Neurosurgery. Springer, Berlin, 2009, pp 1665–1678.
16 Tournier JD, Calamante F, Gadian DG, Connelly A: Direct estimation of the fiber orientation density function from diffusion-weighted MRI data using spherical deconvolution. Neuroimage 2004;23:1176–1185.
17 Tournier JD, Calamante F, Connelly A: Robust determination of the fiber orientation distribution in diffusion MRI: non-negativity constrained super-resolved spherical deconvolution. Neuroimage 2007;35:1459–1472.
18 Calamante F, Tournier JD, Jackson GD, Connelly A: Tract density imaging (TDI): super-resolution white matter imaging using whole-brain tract-density mapping. Neuroimage 2010;53:1233–1243.
19 Garcia-Gomar MG, Concha Luis, Alcauter S, Soto-Abraham J, Carrillo-Ruiz JD, Castro-Farfan G, Velasco-Campos F: Probabilistic tractography of the posterior sub-thalamic area in Parkinson's disease patients. J Bi Sci 2013;6:381–390.
20 Teune LK, Bartels AL, de Jong BM, Willemsem ATM, Eshuis SA, de Vries JJ, van Oostrom JCH, Lenders KI: Typical cerebral metabolic patterns in neurodegenerative brain diseases. Mov Disord 2010;25:2395–2404.
21 Lin TP, Carbon M, Tang C, Magilner AY, Sterio D, Beric A, Dhawan V, Eidelberg D: Metabolic correlates of subthalamic nucleus activity in Parkinson's disease. Brain 2008;131: 1370–1380.
22 Castro G, Carrillo-Ruiz JD, Salcido V, Soto J, García–Gomar G, Velasco AL, Velasco F: Optimizing prelemniscal radiations as a target for motor symptoms in Parkinson's disease treatment. Stereotact Funct Neurosurg 2015; 93:282–291.
23 Gill WM, McIntyre CC: Extracellular excitation of neurons: implications for the mechanisms of deep brain stimulation. Thalamus Relat Syst 2001;1:269–277.
24 Garcia L, Audin J, D'Alessandro G, Bioulac B, Hammond C: Dual effect of high-frequency stimulation on subthalamic neuron activity. J Neurosci 2003;23:8743–8751.
25 Hilker R, Voges J, Weber T, Kracht LW, Roggendorf J, Baudrexel S, Hoevels M, Sturm V, Heiss WD: STN-DBS activates target area in Parkinson's disease. Neurology 2008;71: 708–713.
26 De Long MR: Primate models of movement disorders of basal ganglia origin. Trends Neurosci 1990;13:281–285.
27 Yelnik J: Modeling the organization of the basal ganglia. Rev Neurol (Paris) 2008;164: 969–976.
28 Thobois S, Ballanger B, Xie-Brustolin J, Damier P, Azway JP, Derost P, Witjas T, Raoul S, Le Bas D, Broussolle E: Globus pallidus stimulation reduces frontal hyperactivity in tardive dystonia. J Cereb Blood Flow Metab 2008;28:1127–1138.
29 Feigin A, Fukuda M, Dhawan V, Przedborski S, Jackson-Lewis V, Mentis M, Moeller JR, Eidelberg D: Metabolic correlates of levodopa response in Parkinson's disease. 2001;57: 2083–2088.
30 Haslinger B, Kalteis K, Boecker H, Alesh F, Ceballos-Baumann AO: Frequency-correlated decreases of motor cortex activity associated with subthalamic nucleus stimulation in Parkinson's disease. Neuroimage 2005;28: 598–606.
31 Asanuma K, Tang C, Ma Y, Dhawan V, Mattis P, Edwards CA, Kaplitt M, Feigin A, Eildelberg D: Network modulation in the treatment of Parkinson's disease. Brain 2006;129:2667–2678.
32 Tróst M, Su S, Su PC, Yen RF, Tseng HM, Barnes A, Ma Y, Eidelberg D: Network modulation by the subthalamic nucleus in the treatment of Parkinson's disease. Neuroimage 2006;31:301–307.
33 Cilia R, Marotta G, Landi A, Isaias IU, Mariani CB, Vergani F: Clinical and cerebral activity changes induced by sub-thalamic nucleus stimulation in advanced Parkinson's disease. Clin Neurol Neurosurg 2008;11: 140–146.
34 Karimi M, Goldchin N, Tabbal SD, Hershey T, Videen TO, Wu J, Usche JWM, Revilla FJ, Hartlein JM, Wernle AR, Mink JW, Perlmutter JS: Subthalamic nucleus stimulation-induced regional blood flow responses correlate with improvement of motor signs in Parkinson's disease. Brain 2008;131:2710–2719.
35 Arai N, Yokochi F, Ohnishi T, Momose T, Okiyama R, Taniguchi M, Takahashi H, Matsuda H, Ugawa Y: Mechanisms of unilateral STN-DBS in patients with Parkinson's disease: a PET study. J Neurol 2008;255:1236–1343.
36 Sestini S, Scotto di Lucio A, Ammannati F, De Cristofaro MT, Passeri A, Martini S, Pupi A: Changes in regional blood flow caused by deep brain stimulation of the sub-thalamic nucleus in Parkinson's disease. J Nucl Med 2002;43:725–732.